Contrib Mineral Petrol (2006) 151: 267–281
DOI 10.1007/s00410-005-0050-7

ORIGINAL PAPER

Thomas A. Vogel · Timothy P. Flood
Lina C. Patino · Melissa S. Wilmot
Raymond Patrick R. Maximo · Carmencita B. Arpa
Carlo A. Arcilla · James A. Stimac

Geochemistry of silicic magmas in the Macolod Corridor, SW Luzon, Philippines: evidence of distinct, mantle-derived, crustal sources for silicic magmas

Received: 28 June 2005 / Accepted: 15 November 2005 / Published online: 14 February 2006

Abstract Silicic volcanic deposits (> 65 wt% SiO_2), which occur as domes, lavas and pyroclastic deposits, are relatively abundant in the Macolod Corridor, SW Luzon, Philippines. At Makiling stratovolcano, silicic domes occur along the margins of the volcano and are chemically similar to the silicic lavas that comprise part of the volcano. Pyroclastic flows are associated with the Laguna de Bay Caldera and these are chemically distinct from the domes and lavas at Makiling stratovolcano. As a whole, samples from the Laguna de Bay Caldera contain lower concentrations of MgO and higher concentrations of $Fe_2O_{3(t)}$ than the samples from domes and lavas. The Laguna de Bay samples are more enriched in incompatible trace elements. The silicic rocks from the domes, Makiling Volcano and Laguna de Bay Caldera all contain high alkalis and high K_2O/Na_2O ratios. Melting experiments of primitive basalts and andesites demonstrate that it is difficult to produce high K_2O/Na_2O silicic magmas by fractional crystallization or partial melting of a low K_2O/Na_2O source. However, recent melting experiments (Sisson et al., Contrib Mineral Petrol 148:635–661, 2005) demonstrate that extreme fractional crystallization or partial melting of K-rich basalts can produce these silicic magmas. Our model for the generation of the silicic magmas in the Macolod Corridor requires partial melting of mantle-derived, evolved, moderate to K-rich, crystallized calc-alkaline magmas that ponded and crystallized in the mid-crust. Major and trace element variations, along with oxygen isotopes and ages of the deposits, are consistent with this model.

Electronic Supplementary Material Supplementary material is available for this article at http://dx.doi.org/10.1007/s00410-005-0050-7

Communicated by T. L. Grove

T. A. Vogel (✉) · L. C. Patino · M. S. Wilmot · C. B. Arpa
Department of Geological Sciences, Michigan State University, East Lansing, MI 48824-1115, USA
E-mail: vogel@msu.edu
Tel.: +1-517-3539029
Fax: +1-517-3538787

T. P. Flood
Department of Geology, St. Norbert College, 100 Grant Street, De Pere, WI 54115-2099, USA

R. P. R. Maximo · C. B. Arpa
Philippine Institute of Volcanology and Seismology, Quezon City, Philippines

C. A. Arcilla
University of the Philippines—Diliman, National Institute of Geological Sciences, Quezon City, Philippines

J. A. Stimac
Unocal Philippines, Inc, 12th Floor, Citibank Tower, 1226 Makati City, Philippines

Introduction

The production of silicic magmas in oceanic arc settings, without the involvement of evolved continental crust, has been controversial. Models for the origin of silicic magmas in areas with continental crust involve partial melting or assimilation of crustal rocks (DePaolo 1981; Cobbing and Pitcher 1983; White and Chappell 1983; Hildreth and Moorbath 1988; Vielzeuf and Holloway 1988). On the contrary, silicic magmatism has been considered to be minor in oceanic arcs where evolved continental crust is absent. However, recent works (Tamura and Tatsumi 2002; Leat et al. 2003; Smith et al. 2003; Vogel et al. 2004) have shown that silicic volcanism can be significant in oceanic arcs without old, evolved, continental-like crust. Workers propose that the generation of silicic magmas is due to the partial melting of, or melt extraction from, recently emplaced, mantle-derived, stalled (crystallized or partially crystallized), calc-alkaline magmas. Significantly, the emplacement of silicic magmas in areas without old, evolved crust represents the formation of new continental crust.

The Philippine Archipelago is built upon oceanic arcs with no old, evolved, continental crust, except for the Palawan-Mindoro microcontentinal block to the southwest (Knittel et al. 1988) (Fig. 1). Silicic volcanic deposits (> 65 wt% SiO_2) are relatively abundant in the Macolod Corridor, SW Luzon, Philippines (Figs. 1, 2). They occur as domes on the western and southern flanks of Makiling Volcano, as lava flows associated with Makiling Volcano and as pyroclastic flows and related deposits erupted from Laguna de Bay Caldera (Fig. 3). This paper focuses on the origin of the magmas that produced silicic domes (Fig. 3) and compares them to the lavas at Makiling stratovolcano (J.B. Cruz, unpublished thesis) as well as to the relatively large volume pyroclastic deposits erupted from Laguna de Bay Caldera (Catane and Arpa 1998). These comparisons will be used to constrain genetic models.

Geologic setting

Most of the Philippine Archipelago lies between two opposing subduction systems (Fig. 1). At the latitude of Luzon Island, the Eurasian (Sunda) Plate is being subducted eastward along the Manila Trench (Cardwell et al. 1980), whereas the Philippine Sea Plate is undergoing a westward subduction along the Philippine Trench. The Luzon Arc is the product of eastward subduction and has been divided into two segments, the Bataan Arc to the north and the Mindoro Arc to the south based on distinctive geochemical and isotopic trends in recent volcanic rocks (Defant et al. 1988). The Macolod Corridor is a NE-trending, 80 km wide zone of extensional faulting between these two segments of the Luzon Arc (Sudo et al. 2001) that is nearly perpendicular

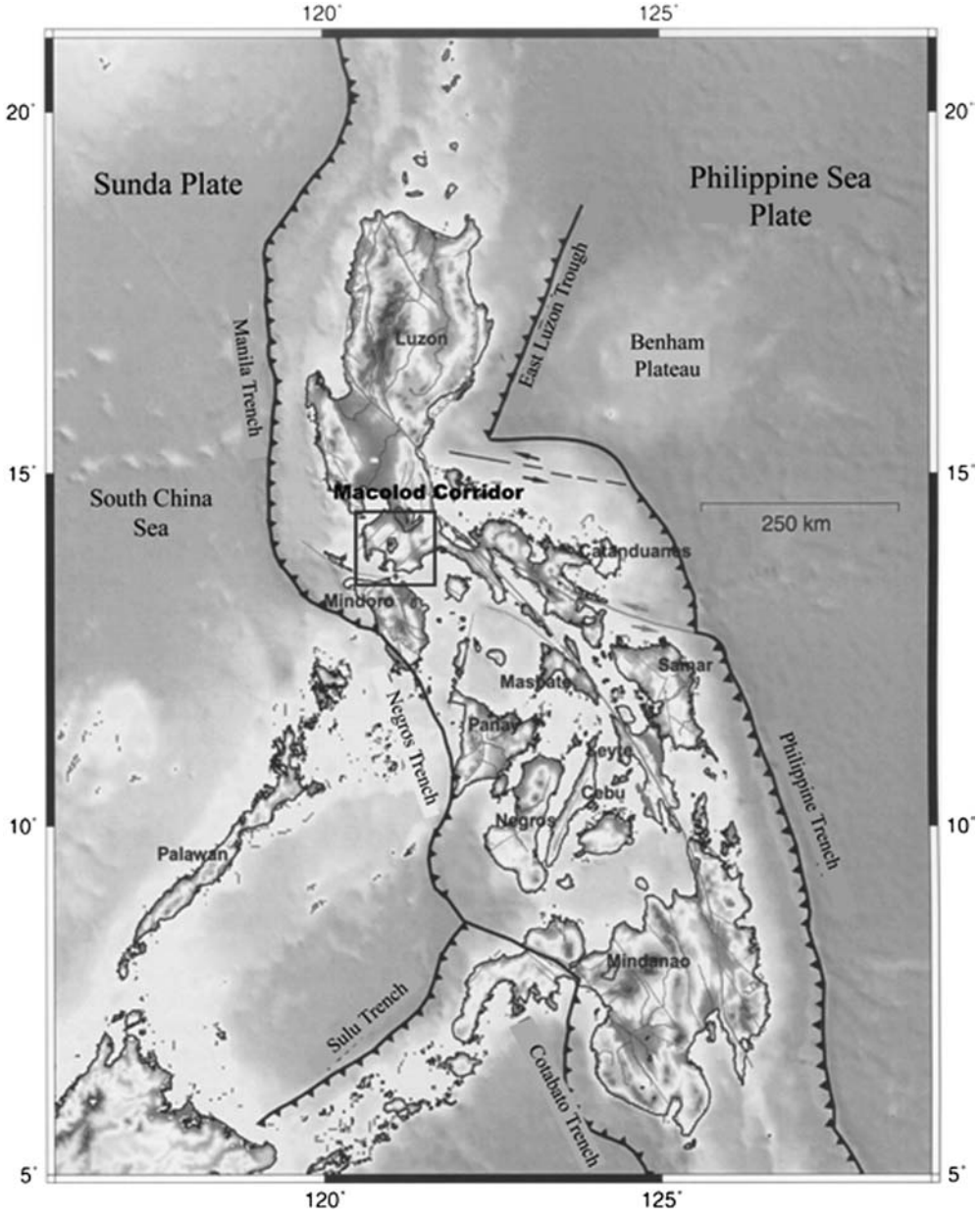

Fig. 1 Tectonic map of the Philippine Archipelago, showing the setting of the Macolod Corridor (Bacolcol 2003). *Close triangles* are volcanoes; *hachures* on faults indicate downthrown block; *large arrows* indicate opening direction of Macolod Corridor

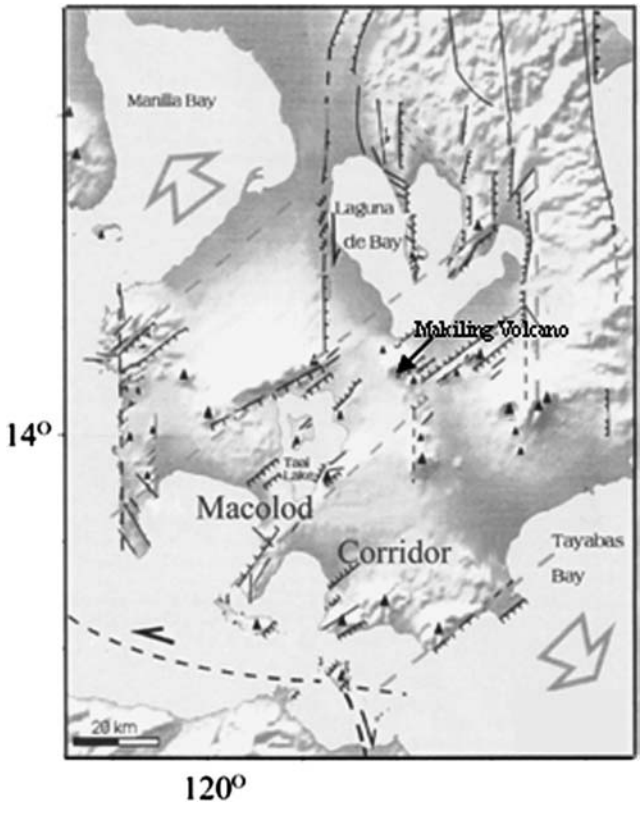

Fig. 2 Simplified geologic map of the Macolod Corridor. *Triangles* are volcanoes or volcanic centers. Faults are represented by *hachured lines* (*hachures* indicate the downthrown area), *open arrows* point to the inferred direction of minimum horizontal stress and ongoing extension of the Macolod Corridor. Laguna de Bay Caldera is the middle lobe of Laguna de Bay (Le Rouzic 1999)

to the arc front (Figs. 1, 2). The Macolod Corridor is also characterized by intense Pleistocene to Holocene volcanism. Sets of NE–SW and N–S trending faults and fractures are the dominant structural elements of the Macolod Corridor, but NW–SE trending structures parallel to the arc are also present (Fig. 2; Förster et al. 1990; Pubellier et al. 2000; Aquino 2004).

The crustal structure of the Luzon Arc is not well known. Based on receiver functions in the vicinity of Taal Volcano, which is located on the northern edge of the Macolod Corridor, Besana et al. (1995) suggested that the crust at this location is 34 km thick (Besana et al. 1995). Their shear-wave velocity model is complex with a thick, low-velocity zone at about 18 km, underlain by alternating low- and high-velocity zones. They interpret the 4 km thick low-velocity zone at 18 km due to partial melt and the alternating low- and high-velocity zones due to a complex lower crust.

The origin of the Macolod Corridor is still a matter of debate, and various hypotheses have been proposed. Defant et al. (1988) and many later workers have argued for a pull-apart rift zone, whereas Förster et al. (1990) suggested a pull-apart structure due to a diffuse system of NW–SE oriented shears. Rifting due to transtensional motion has been proposed for the origin of the Macolod Corridor (Pubellier et al. 2000; Aquino 2004) although the general consensus is that it is a pull-apart rift zone. Adjacent to the Macolod Corridor is a sequence of Paleocene–Oligocene San Juan metavolcanics and metasediments and early to mid-Miocene San Juan quartz diorite (Oles 1991; Sudo et al. 2001).

Volcanic centers within the Macolod Corridor consist of two large volcano–tectonic depressions (Taal and Laguna de Bay Calderas), three stratovolcanoes (Makiling, Cristo and Banahaw) and more than 200 small monogenetic volcanic scoria cones, domes and maars (Förster et al. 1990) (Fig. 2). The Laguna de Bay Caldera is a 200 km^2 depression that forms the central lobe of a large, three-fingered lake called Laguna de Bay (Fig. 2). This caldera has erupted large volumes of pyroclastic material, with reported ages from about 27 to about 50 ka (Catane and Arpa 1998; Arpa et al. 1999a; Catane et al. 2004). Although the volume of erupted products has not been determined, the caldera is 15×30 km^2 (Arpa et al. 1999b) and pyroclastic units from this caldera have been observed in metro Manila, 40 km to the northwest. Abundant fresh outcrops are observed in quarries in the immediate vicinity of the caldera, but outcrops are poor, due to weathering, where quarries are absent. Based on our chemical analyses of pumice fragments, the pyroclastic deposits range in composition from 53 to 69 wt% SiO_2. The Makiling volcanic complex is composed of lava flows, coalesced domes and pyroclastic deposits (Fig. 3), primarily of basaltic andesite and andesite composition with lesser amounts of trachyandesite and dacite (J.B. Cruz, unpublished thesis).

The initiation of the most recent episodes of volcanism in the Macolod Corridor is not well constrained, with estimates ranging from 1.8 to 0.6 Ma (Sudo et al. 2001). Volcanism continues through the present (Defant et al. 1989; Sudo et al. 2001), with the most recent pyroclastic eruptions occurring at Taal Volcano approximately 5 ka (Listanco 1994; Martinez and Williams 1999). The most recent eruption of lava from Taal was in 1977 (Miklius et al. 1991).

Sampling

Silicic domes

At least seven silicic domes are present near the western and southeastern flanks of Mt. Makiling Volcano (Fig. 3). Six of these [Mt. Bijang, Calamba (Mt. Mapinggoy), Turupiche (Tanauan Hill), San Antonio, Olila and Bulalo] were sampled for this study. Bulalo and Olila Domes are near the site of the Mak-Ban geothermal field, a commercial field, operated by Unocal Philippines Incorporated (UPI). Drilling data from this field reveal that continuous hornblende dacite lavas similar to the Bulalo and Olila Dome compositions underlie at least 10 km^2 on the southeast flank of Mt. Makiling with a thickness varying from about 30 to

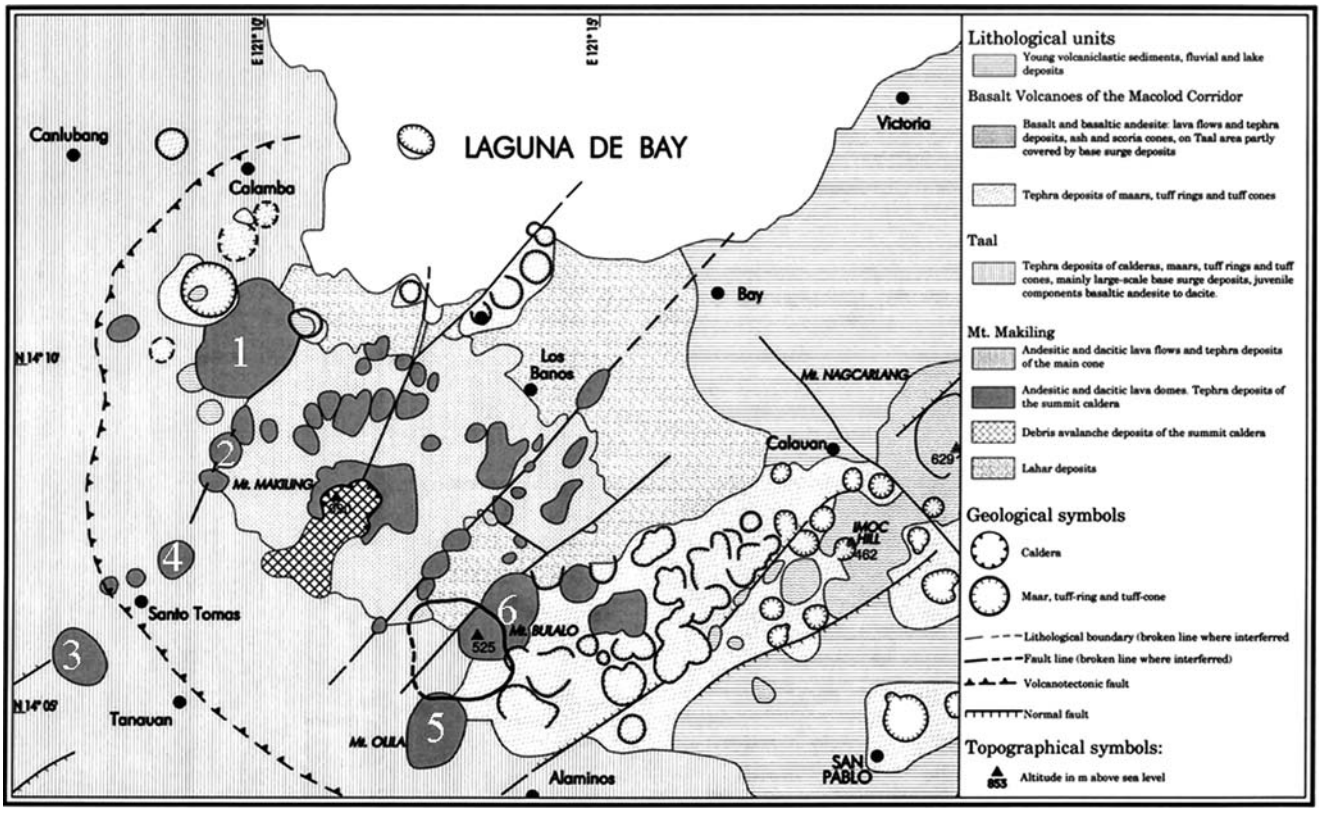

Fig. 3 Simplified geologic map of Makiling Volcano (modified from Oles 1991) showing the distribution of the domes around the volcano. The domes are labeled as: *1* Bijang, *2* Calamba, *3* Turupiche (Tanauan Hill), *4* San Antonio, *5* Olila and *6* Bulalo

about 200 m. These units are buried by alluvium and younger pyroclastic deposits from Taal.

The least altered samples of the domes were obtained at recent road cuts or active construction sites (Mt. Bijang, Bulalo and Olila) and quarries (Calamba). Where recent construction sites do not exist (Turupiche and San Antonio Domes), fresh samples were difficult to obtain due to deep tropical weathering. Fewer samples were obtained from these domes.

Ignimbrites

The Laguna de Bay Caldera produced voluminous pyroclastic flow deposits that were directed mostly to the northwest and north (Arpa et al. 1999a) and are well exposed in active quarries, construction sites and road cuts with 15 km of the margin of the caldera. Detailed descriptions of these pyroclastic deposits are beyond the scope of this paper—based on our studies, they are composed of at least three eruptive units that contain heterogeneous assemblages of pumice fragments. Samples of glassy pumice fragments were obtained from 31 different sites that were distributed throughout the area. Based on crystal content, color and vesiculation, all megascopically distinct pumice varieties were collected.

Chemical analyses

For the pyroclastic deposits, pumice samples were analyzed. For the domes, where possible, the host rocks were separated from the enclaves—enclaves that were large enough were analyzed separately. When necessary samples were cleaned, passed through a chipmunk rock crusher and powdered using a ceramic flat plate grinder. Three grams of this rock powder and 9.0 g of lithium tetraborate ($Li_2B_4O_7$), along with 0.5 g of ammonium nitrate (NH_4NO_3) (as an oxidizer) were fused in platinum crucibles at 1,000°C for 20–30 min on an orbital mixing stage. The melt was then poured into platinum molds making the glass disk that was analyzed using a Rigaku S-Max X-ray fluorescent (XRF) spectrograph. XRF major element analyses were reduced by a fundamental parameter data reduction method using XRF-WIN® software (Omni Instruments), while XRF trace element data were calculated using standard linear regression techniques. All major and trace element whole rock analyses were done at the Michigan State University. Major elements and Rb, Sr and Zr were analyzed using XRF. The rare earth elements, Nb, Ta, Hf, Ba, Y, Th, U and Pb, were analyzed by laser ablation inductively coupled plasma mass spectrometry on the same glass disks as used for XRF analyses. A Cetac LSX200+ laser ablation system was used coupled with a Micromass Platform ICP-MS, using strontium,

determined by XRF, as an internal standard. Trace element data reduction was done using MassLynx software. Element concentrations in the samples were calculated based on a linear regression method using well-characterized standards. Table 1 represents the precision and accuracy of chemical analyses done in our laboratory by replicating analyses of a standard (Jb-1a). Representative chemical analyses of the domes are given in Tables 2 and 3.

Oxygen isotope data for mineral separates from Calamba, Bulalo and Bijang Domes were collected using the CO_2 laser fluorination/mass spectrometer at the University of Wisconsin-Madison (Table 4). Values represent averages of 2–4 individual analyses on different separates from the same sample. Oxygen was liberated from 1 to 3 mg of silicate and oxide by CO_2 laser fluorination and analyzed on a Finnigan MAT-251 gas-source isotope-ratio mass spectrometer (Valley et al. 1995).

$^{40}Ar/^{39}Ar$ ages were determined in samples from five domes (Mt. Bijang, Calamba, Tanauan Hill, Olila and Mt. Bulalo Domes) at the New Mexico Geochronological Research Laboratory (Table 5). Hornblende separates were analyzed by the incremental step heating method for all domes except Calamba, which contains only trace amounts of hornblende. Because the Calamba

Table 1 JB-1a treated as an unknown for XRF and ICP-MS analyses: five different sample preparations

Variable	*N*	Mean	Median	SD	SE[a]	Given[b]
XRF data						
SiO_2	5	52.05	52.16	0.273	0.122	52.41
TiO_2	5	1.28	1.28	0.005	0.002	1.32
Al_2O_3	5	14.50	14.5	0.036	0.016	14.53
$Fe_2O_{3(t)}$	5	9.00	9	0.005	0.002	9.05
MnO	5	0.14	0.14	0.000	0.000	0.15
MgO	5	7.82	7.81	0.069	0.031	7.83
CaO	5	9.29	9.29	0.008	0.004	9.31
Na_2O	5	2.71	2.71	0.023	0.010	2.73
K_2O	5	1.38	1.38	0.005	0.002	1.40
P_2O_5	5	0.27	0.27	0.004	0.002	0.26
Total	5	98.45	98.49	0.171	0.076	98.99
Cr	5	373	372	6	3	392
Ni	5	138	138	2	1	139
Cu	5	74	75	6	3	57
Zn	5	74	74	1	0	82
Rb	5	40	41	2	1	39
Sr	5	460	460	2	1	442
Y	5	23	23	1	0	24
Zr	5	139	139	1	0	144
Nb	5	22	22	1	0	27
La	5	27	29	6	3	38
Ba	5	455	461	22	10	504
ICP-MS data						
Zr	5	147.13	147.33	1.97	0.88	144
Ba	5	473.72	475.75	5.74	2.57	504
La	5	38.24	38.32	0.48	0.22	37.6
Ce	5	62.63	63.16	1.25	0.56	65.9
Pr	5	7.29	7.39	0.25	0.11	7.3
Nd	5	27.36	27.57	0.82	0.36	26.9
Sm	5	5.47	5.52	0.20	0.09	5.07
Eu	5	1.54	1.55	0.07	0.03	1.46
Gd	5	5.08	5.13	0.14	0.06	4.67
Tb	5	0.79	0.8	0.02	0.01	0.69
Y	5	24.57	24.55	0.17	0.08	24
Dy	5	4.25	4.28	0.09	0.04	3.99
Ho	5	0.83	0.84	0.03	0.01	0.71
Er	5	2.30	2.31	0.07	0.03	2.18
Yb	5	2.27	2.29	0.09	0.04	2.1
Lu	5	0.33	0.34	0.01	0.01	0.33
V	5	186.88	186.39	3.49	1.56	205
Cr	5	380.92	377.91	8.72	3.90	392
Nb	5	27.21	26.98	0.67	0.30	26.9
Hf	5	3.73	3.78	0.18	0.08	6.65
Ta	5	1.83	1.86	0.08	0.04	1.93
Pb	5	5.85	5.92	0.18	0.08	6.76
Th	5	10.02	10.11	0.36	0.16	9.03
U	5	1.64	1.67	0.07	0.03	1.67

[a]Standard error = standard deviation divided by the square root of the number of samples
[b]http://www.aist.go.jp/RIODB/geostand/igneous.html

Table 2 Representative major element analyses (in wt%) of hosts and enclaves from domes

Sample	Dome	Lon(N)	Lat(E)	SiO_2	TiO_2	Al_2O_3	$Fe_2O_{3(t)}$	MnO	MgO	CaO	Na_2O	K_2O	P_2O_5	Totals
Sample	Calamba	14.144	121.162	53.28	0.81	18.11	7.85	0.15	4.15	8.95	3.37	1.48	0.16	98.31
17-2a	Calamba			65.10	0.65	16.03	4.41	0.10	1.33	3.76	4.28	2.97	0.16	98.79
17-2b	Calamba			50.96	0.89	17.99	9.10	0.15	5.24	10.38	3.00	0.90	0.14	98.75
17-2c	Calamba			52.44	0.97	17.67	9.08	0.16	4.43	8.99	3.31	1.23	0.16	98.44
17-2e	Calamba			65.51	0.66	15.98	4.47	0.10	1.28	3.65	4.27	3.01	0.17	99.10
17-2f	Calamba			64.61	0.64	16.23	4.35	0.10	1.34	3.76	4.29	2.94	0.16	98.42
17-2g	Calamba			66.19	0.64	16.07	4.36	0.10	1.31	3.81	4.22	2.97	0.16	99.83
17-2h	Calamba			64.64	0.69	15.90	4.74	0.11	1.39	3.80	4.23	2.93	0.16	98.59
17-2i	Calamba			65.58	0.66	15.81	4.46	0.11	1.43	3.52	4.22	3.16	0.16	99.11
15-3B	Mt. Bijang	14.163	121.166	69.10	0.37	14.56	2.94	0.08	0.88	2.73	3.66	3.45	0.10	97.87
18-1a	Mt. Bijang			68.60	0.37	14.77	2.93	0.08	0.91	2.68	3.60	3.49	0.10	97.53
18-1TAV-a	Mt. Bijang			67.40	0.38	15.08	3.05	0.08	1.00	2.89	3.36	3.74	0.10	97.08
18-1TAV-b	Mt. Bijang			68.92	0.36	14.65	2.75	0.08	0.88	2.64	3.63	3.44	0.10	97.45
18-1TAV-c	Mt. Bijang			67.89	0.38	14.85	2.90	0.08	0.92	2.67	3.68	3.49	0.10	96.96
18-1f	Mt. Bijang			68.82	0.37	14.53	2.91	0.08	0.89	2.62	3.46	3.86	0.10	97.64
18-1g	Mt. Bijang			68.07	0.40	14.63	3.23	0.09	0.98	2.71	3.61	3.51	0.10	97.33
18-1h	Mt. Bijang			69.00	0.39	14.66	3.11	0.08	0.91	2.60	3.55	3.69	0.11	98.10
15-4A	Mt. Bijang			69.03	0.37	14.69	2.78	0.08	0.92	2.68	3.67	3.54	0.11	97.87
15-4B	Tanauan Hill	14.091	121.129	67.08	0.41	15.04	3.27	0.09	1.01	2.92	3.85	3.46	0.12	97.25
18-2a	Tanauan Hill			69.13	0.38	14.59	2.99	0.09	0.88	2.69	3.71	3.61	0.11	98.18
18-2b	Tanauan Hill			68.07	0.42	14.90	3.49	0.10	1.02	3.01	3.78	3.40	0.12	98.31
18-2c	Tanauan Hill			68.32	0.37	14.61	2.81	0.09	0.80	2.47	3.87	3.51	0.11	96.96
20-1a	Tanauan Hill			68.62	0.38	14.85	2.88	0.09	0.85	2.65	3.92	3.39	0.11	97.74
20-1b	Tanauan Hill			68.43	0.38	14.70	2.91	0.09	0.85	2.57	3.79	3.62	0.11	97.45
20-1c	Mt. Bulalo	14.110	121.209	69.78	0.37	14.37	2.84	0.09	0.80	2.39	3.76	3.60	0.11	98.11
22-50TAV	Mt. Bulalo			49.87	1.06	17.82	10.66	0.18	4.32	9.67	3.10	1.02	0.21	97.91
22-51TAV	Mt. Bulalo			50.71	1.03	17.75	10.20	0.18	4.19	9.27	3.11	1.14	0.21	97.79
22-51tavE1	Mt. Bulalo			51.28	1.04	17.69	10.31	0.18	4.03	9.29	3.13	1.16	0.21	98.32
22-51tavE2	Mt. Bulalo			68.54	0.40	15.62	3.18	0.10	1.02	2.98	4.32	3.03	0.12	99.31
15-1A	Mt. Bulalo			68.95	0.40	15.37	3.11	0.10	1.05	2.95	4.32	3.07	0.13	99.45
15-1B	Mt. Olila	14.082	121.211	52.52	0.85	17.65	9.29	0.17	4.36	8.83	2.97	1.29	0.21	98.14
22-52TAV	Mt. Olila			70.04	0.38	14.99	2.88	0.09	0.88	2.78	4.00	3.20	0.13	99.37
22-53TAV	Mt. Olila			68.82	0.39	15.14	2.88	0.09	0.90	2.69	4.14	3.19	0.12	98.36
22-54TAV	Mt. Olila			69.64	0.37	14.84	2.80	0.09	0.86	2.64	4.07	3.24	0.11	98.66
22-55TAV	Mt. Olila			69.09	0.38	15.24	2.90	0.09	0.90	2.92	4.12	3.16	0.13	98.93

Dome rock lacked hornblende, plagioclase was analyzed. The methods used can be found at http://www.geoinfo.nmt.edu/publications/openfile/argon/home.html. Because of the young age of the samples, large amounts of hornblende (~50–115 mg) were analyzed. Two samples, one from Bulalo Dome and one from Olila Dome, were replicated four times each to assess age homogeneity and to improve overall precision. Typically, 6–8 heating steps were used to construct the age spectra (data are available from the corresponding author upon request).

Minerals were analyzed using a Cameca SX 100 EMPA at the University of Michigan. In general, an accelerating potential of 15 kV was used. Other settings such as beam spot size, counting time, and current varied based on the phase being analyzed.

Texture and mineralogy of the domes

The mineral assemblages of the domes are very similar with the exception of Calamba. All dome samples contain 15–25% phenocrysts. The dominant phase is plagioclase followed by hornblende, except in the Calamba Dome where orthopyroxene and clinopyroxene are the mafic phases. Samples taken from surface exposures of domes are glassy and microlitic in all the domes except Calamba, where some samples are devitrified. Mafic enclaves are found in most domes, but none were observed in the Bijang Dome. Mafic enclaves vary in size from about 1 to 25 cm. Based on the limited outcrops, the abundance of these enclaves is generally about 5%, but locally it is as much as 20% in some quarry exposures in the Calamba Dome. The major differences between the large and small enclaves are the size of the grains in the enclaves and the textural evidence of interaction with the host magma. Some large enclaves exhibit crenulate chill margins and vesicular interiors, whereas small enclaves have interacted with the host magma.

The domes, except for Calamba Dome, contain plagioclase, hornblende and orthopyroxene in the order of decreasing abundance, along with some trace phases. For Calamba Dome, the order of abundance is plagioclase, orthopyroxene, clinopyroxene, with minor amounts of hornblende. Plagioclase compositions in the domes are similar. Anorthite content decreases towards the edges of the grains with the edge composition ranging from An_{31} to An_{41}. Plagioclase cores generally contain a maximum anorthite content of An_{55}. Centers

Table 3 Representative trace element analyses (in ppm) of hosts and enclaves from domes

Sample	Dome	Rb	Sr	Zr	V	Cr	Y	Nb	Ba	La	Ce	Pr	Nd	Sm	Eu	Gd	Tb	Dy	Ho	Er	Yb	Lu	Hf	Ta	Pb	Th	U
17-2a	Calamba	36	522	83	245	45	19	5	357	15	29	3.6	14.6	3.4	1.2	3.4	0.5	3.1	0.7	1.9	2.0	0.3	2.1	0.3	8	4.6	1.0
17-2b	Calamba	74	341	185	103	6	25	9	650	24	49	5.6	20.9	4.5	1.2	4.4	0.7	3.9	0.8	2.5	2.9	0.4	4.5	0.5	12	10.3	3.1
17-2c	Calamba	20	535	61	277	64	18	4	263	11	22	2.8	11.8	2.9	1.0	3.1	0.5	2.9	0.6	1.7	1.8	0.3	1.6	0.2	6	3.0	0.7
17-2e	Calamba	26	523	80	277	17	21	5	304	13	25	3.2	13.6	3.2	1.1	3.4	0.5	3.2	0.7	2.1	2.1	0.3	2.2	0.3	8	4.0	0.8
17-2f	Calamba	69	335	196	103	5	26	10	666	24	50	5.8	21.7	4.7	1.2	4.5	0.7	4.0	0.9	2.5	3.0	0.4	4.6	0.5	14	10.1	3.2
17-2g	Calamba	72	352	193	105	6	24	10	672	24	49	5.6	21.2	4.5	1.3	4.5	0.7	4.3	0.9	2.6	2.9	0.4	4.8	0.7	13	11.4	4.3
17-2h	Calamba	75	344	191	105	5	23	10	670	23	49	5.5	20.3	4.3	1.2	4.3	0.7	3.6	0.8	2.2	2.5	0.4	4.4	0.6	17	11.0	4.3
17-2i	Calamba	73	342	192	121	6	23	11	667	24	50	5.8	21.4	4.6	1.3	4.6	0.7	3.8	0.8	2.4	2.8	0.4	4.7	0.6	18	11.0	4.3
15-3B	Calamba	80	319	203	125	8	25	11	693	23	52	5.5	20.6	9.6	1.2	4.3	0.7	3.9	0.9	2.6	2.7	0.4	4.3	0.6	23	10.5	3.5
18-1a	Mt. Bijang	95	307	160	70	6	13	9	780	23	42	4.1	13.4	2.7	0.7	2.6	0.4	2.1	0.4	1.3	1.8	0.3	3.8	0.6	35	15.3	6.0
18-1TAV-a	Mt. Bijang	93	309	168	69	7	12	9	779	22	41	4.1	13.6	2.7	0.8	2.5	0.3	2.1	0.4	1.3	1.6	0.3	3.9	0.7	22	14.1	6.0
18-1TAV-b	Mt. Bijang	90	327	164	71	6	13	9	762	23	42	4.3	14.8	2.8	0.8	2.7	0.4	2.1	0.5	1.4	1.9	0.3	4.1	0.7	37	16.5	5.7
18-1TAV-c	Mt. Bijang	96	302	163	60	6	13	8	797	23	42	4.2	13.8	2.5	0.8	2.5	0.4	1.9	0.4	1.3	1.7	0.2	4.0	0.6	36	15.8	5.8
18-1f	Mt. Bijang	89	315	170	68	7	12	9	766	22	41	4.1	13.5	2.4	0.8	2.5	0.4	2.0	0.5	1.4	1.7	0.3	4.1	0.7	24	15.2	6.0
18-1g	Mt. Bijang	96	297	159	65	5	12	9	776	22	41	4.0	13.2	2.5	0.8	2.6	0.4	1.9	0.5	1.3	1.6	0.3	3.9	0.7	35	15.7	5.8
18-1h	Mt. Bijang	92	305	162	81	6	13	9	776	23	43	4.3	14.4	2.9	0.8	2.8	0.4	2.1	0.5	1.5	1.8	0.3	4.1	0.7	36	16.1	6.1
15-4A	Mt. Bijang	107	304	167	76	7	12	9	817	22	45	4.2	13.4	2.5	0.8	2.6	0.4	2.0	0.5	1.5	1.6	0.2	3.8	0.7	33	15.9	4.6
15-4B	Mt. Bijang	99	310	163	64	6	13	9	814	22	45	4.3	13.8	2.6	0.8	2.7	0.5	2.1	0.5	1.5	1.7	0.2	3.6	0.7	33	15.5	4.5
18-2a	Tanauan Hill	87	325	159	71	4	14	8	772	23	42	4.3	14.0	2.8	0.9	2.8	0.4	2.1	0.5	1.4	1.7	0.3	3.6	0.5	31	14.2	5.3
18-2b	Tanauan Hill	93	299	161	908	998	46	2	19	2	5	1.0	6.8	3.1	1.5	5.0	1.0	7.4	1.7	5.0	4.9	0.8	1.9	0.2	9	0.1	0.1
18-2c	Tanauan Hill	81	324	157	76	5	14	8	756	23	42	4.2	14.3	2.6	0.9	2.7	0.4	2.2	0.5	1.5	1.9	0.3	3.7	0.6	29	14.3	5.2
20-1a	Tanauan Hill	95	287	169	60	4	12	7	676	20	38	3.8	13.0	2.6	0.8	2.6	0.4	1.9	0.4	1.3	1.8	0.3	3.4	0.5	29	13.0	4.7
20-1b	Tanauan Hill	95	306	163	58	5	14	8	801	23	43	4.2	13.8	2.5	0.8	2.6	0.4	1.9	0.4	1.3	1.9	0.3	3.6	0.6	27	13.5	4.4
20-1c	Tanauan Hill	96	299	167	63	4	12	7	671	20	37	3.7	12.7	2.4	0.8	2.5	0.4	2.0	0.5	1.4	1.5	0.2	3.3	0.5	28	12.9	4.8
22-50TAV	Mt. Bulalo	90	269	174	185	49	14	3	149	7	13	1.7	7.5	1.9	0.7	2.1	0.4	2.4	0.5	1.4	1.3	0.2	1.4	0.2	6	2.2	0.7
22-51TAV	Mt. Bulalo	23	597	82	125	11	29	18	1,828	53	91	9.3	31.4	5.4	1.7	5.7	0.8	5.2	1.0	3.2	3.8	0.7	10.2	1.8	49	35.6	12.2
22-51tavE1	Mt. Bulalo	31	584	89	352	5	22	3	317	14	27	3.7	16.8	3.9	1.3	4.1	0.6	3.9	0.8	2.2	2.2	0.3	2.3	0.2	6	3.8	0.9
22-51tavE2	Mt. Bulalo	28	586	86	348	6	23	4	353	15	28	4.0	17.3	4.0	1.4	4.4	0.7	4.0	0.8	2.3	2.2	0.4	2.7	0.3	6	4.5	1.3
15-1A	Mt. Bulalo	81	339	170	79	9	13	10	843	23	47	4.4	14.3	2.8	1.0	2.8	0.5	2.1	0.5	1.5	1.7	0.3	3.5	0.7	34	14.1	4.8
15-1B	Mt. Bulalo	85	332	168	65	7	14	8	841	23	45	4.3	14.7	2.9	0.9	2.9	0.5	2.5	0.6	1.7	2.0	0.3	4.0	0.7	34	16.7	4.4
22-52TAV	Mt. Olila	31	504	87	287	3	20	3	291	13	24	3.3	15.0	3.6	1.2	3.7	0.6	3.5	0.7	1.9	1.9	0.3	2.2	0.2	7	3.7	0.9
22-53TAV	Mt. Olila	86	310	181	180	13	12	2	211	8	15	2.0	8.4	2.0	0.7	2.1	0.3	2.2	0.4	1.2	1.2	0.2	1.5	0.2	5	3.0	0.8
22-54TAV	Mt. Olila	86	307	183	54	5	13	8	794	24	42	4.3	15.2	2.6	0.9	2.7	0.4	2.5	0.5	1.5	1.8	0.3	4.2	0.7	22	14.8	5.1
22-55TAV	Mt. Olila	86	295	173	57	5	13	8	802	23	41	4.1	13.9	2.5	0.8	2.6	0.4	2.4	0.5	1.4	1.6	0.3	4.3	0.7	23	14.5	5.2
22-56TAV	Mt. Olila	80	323	165	60	6	14	9	885	26	45	4.6	15.8	2.9	0.9	2.8	0.4	2.6	0.5	1.7	2.0	0.4	4.6	0.8	25	16.5	5.9

Table 4 Data for oxygen isotope calculations of the domes. Oxygen isotope data presented in δ notation (‰) relative to V-SMOW

	Bulalo	Calamba	Bijang
SiO_2 (wt%)	68.5	65.5	68.5
Magnetite δ	2.36 ± 0.08	2.83 (1 analysis)	2.48 ± 0.12
Hornblende δ	4.90 ± 0.03	4.82 ± 0.14	4.67 ± 0.06
Difference δ	2.54	1.99	2.19
Calculated whole rock δ	5.90	6.29	6.06
T (clinopyroxene–magnetite)[a]	908°C	1,060°C	999°C
Δ(melt–amphibole)[b]	1.96	1.28	1.96
Melt $\delta^{18}O‰$ [c]	6.36	6.1	6.13

Values are averages for duplicate analyses. Errors are one standard deviation. See text for discussion
[a]Calculated using the A factor from Chiba et al. (1989)
[b]Δ(melt–amphibole) = 0.61(SiO_2 wt%) − 2.72 (Bindeman et al. 2004)
[c]$\delta^{18}O‰$ melt = $\delta^{18}O‰$ Cpx + Δ(melt–amphibole) (Bindeman et al. 2004)

of some plagioclase grains are as high as An_{84}. Some plagioclase grains contain reverse zoning. Orthopyroxenes in all domes are similar in composition ($Wo_{1.3–3.9}En_{68.4–70.6}Fs_{27.5–29.9}$). Hornblendes compose 25–30% of the phenocrysts assemblage and have little compositional variation among domes (typical hornblende formula of $(Na_{0.07}K_{0.43})Ca_{1.68}(Mg_{3.28}Mn_{0.08}Fe_{0.82}Ti_{0.22}Fe_{0.56}Al_{0.37})[Si_{6.13}Al_{1.87}O_{22}](OH)_2$). The Calamba Dome contains both orthopyroxene and clinopyroxene ($Wo_{40.7–43.4}En_{43.2–45.3}Fs_{13.0–15.0}$) as the dominant mafic phase in subequal amounts. The most abundant accessory phases in the domes are Fe–Ti oxides; only magnetite occurs in most domes, while both magnetite and ilmentite occurs in Calamba Dome. Zircon and apatite occur as trace phases in all domes. All the phases are unaltered.

Mineralogy of the Laguna de Bay pyroclastic deposits

Pumice clasts within the ignimbrites from the Laguna de Bay Caldera are nearly aphyric, containing less than 10% phenocrysts. The dominant phases are plagioclase, orthopyroxene and clinopyroxene. Hornblende occurs in some of the silicic samples. Details of the variations of the mineralogy among the ignimbrite units are beyond the scope of this paper and will be presented in a subsequent paper. The silicic samples contain only orthopyroxene whereas the more mafic samples contain both orthopyroxene and clinopyroxene. Magnetite is the only oxide and trace amounts of apatite and zircon are present.

The mineral compositions are similar to those observed in the domes. Plagioclase rim compositions are similar to the plagioclase from the domes (An_{35}). Clinopyroxene compositions are $Wo_{38–45}En_{41–46}Fs_{14–15}$. Orthopyroxene compositions are $Wo_{3–4}En_{66–70}Fs_{26–30}$.

Chemistry of the domes compared to Makiling lavas and Laguna de Bay ignimbrites

Representative chemical analyses for the domes are given in Tables 2 and 3. A complete data file is given as an electronic supplement. With the exception of Calamba, the domes are dominated by compositions straddling from the dacitic to rhyolitic transition. Glassy matrix is present at all domes, indicating that the rapidly quenched dome carapace has not been removed by erosion. Mafic enclaves are present in three of the domes: Olila, Bulalo and Calamba. The host compositions of all the domes are similar except for Calamba. The host compositions of these domes range from 67.1 to 71.1 wt% SiO_2, with a mean of 70.0 wt% (SD 0.77), whereas the host composition of the Calamba Dome ranges from

Table 5 Summary of $^{40}Ar/^{39}Ar$ hornblende results

Sample	Irrad	N	K/Ca	Age (ka)	± 1σ	Eruption age ± 1σ
Bulalo						
BD-1A-a	NM-155	5	0.052	0.035	0.020	
BD-1A-b	NM-155	2	0.052	0.014	0.013	
BD-1A-c	NM-155	5	0.076	0.015	0.013	
BD-1A-d	NM-155	6	0.084	0.005	0.014	15 ± 7 ka
Bulalo						
BD-1B	NM-155	6	0.148	0.046	0.009	46 ± 9 ka
Olila						
020522-56 TVA-a	NM-163	4	0.053	0.030	0.015	
020522-56 TVA-b	NM-163	4	0.052	-0.009	0.019	
020522-56 TVA-c	NM-163	3	0.053	0.024	0.014	
020522-56 TVA-d	NM-163	3	0.052	-0.042	0.024	11 ± 8 ka
Bijang						
020518-1g	NM-163	2	0.046	0.066	0.014	66 ± 14[a]
Tanauan Hill						
020520-1c	NM-163	4	0.051	0.043	0.017	43 ± 17

N number of steps defining plateau
[a]Maximum age

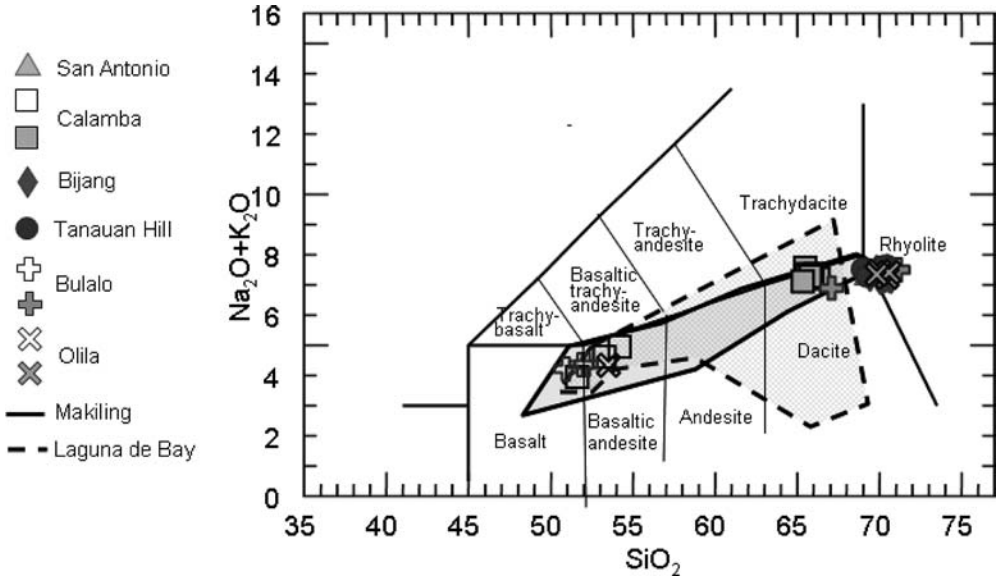

Fig. 4 Alkali–silica classification diagram (LeBas et al. 1986) showing the composition of the domes compared to the lavas of Makiling Volcano. *Dashed line* outlines Laguna de Bay samples; *solid line* outlines Makiling Volcano samples. *Empty symbols* are enclaves

65.3 to 66.3 wt% SiO_2, with a mean of 65.8 wt% (SD 0.32). Mafic enclaves have similar compositions in all domes where they occur and range from 50.9 to 54.2 wt% with a mean of 52.2 wt% (SD 1.18). The host samples plot in the dacite–rhyolite fields and the mafic enclaves plot in the basalt–basaltic andesite fields (LeBas et al. 1986; Fig. 4). Examples of the chemical variation of the domes compared to Makiling lavas and pumice fragments from Laguna de Bay ignimbrites are shown in Figs. 4, 5, 6 and 7.

Chemical analyses of Makiling Volcano are from an unpublished masters thesis of J.B. Cruz, unpublished

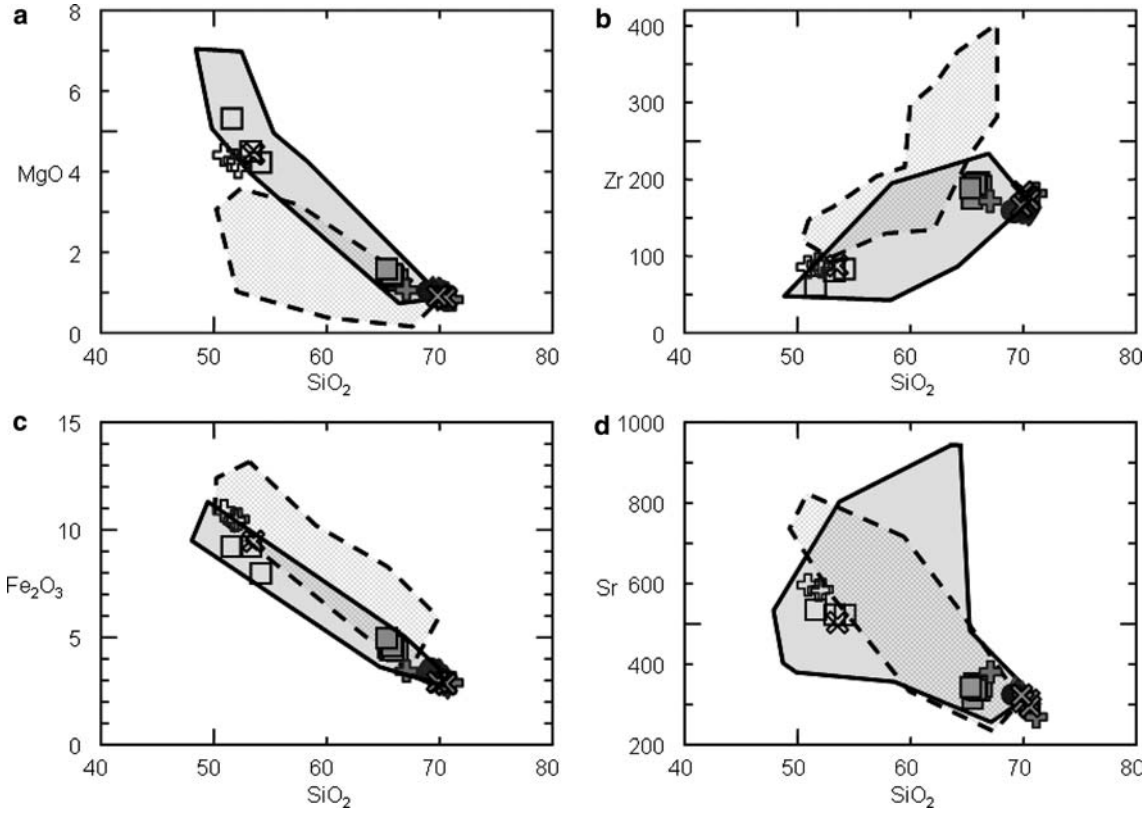

Fig. 5 Chemical comparison of the domes with Makiling lavas and pumice samples from Laguna de Bay ignimbrites. **a** MgO (wt%), **b** Zr (ppm), **c** Fe_2O_3 (wt%) and **d** Sr (ppm) versus SiO_2 (wt%). *Dashed line* outlines Laguna de Bay samples; *solid line* outlines Makiling Volcano samples. Note the general similarities of the dome samples and silicic lava samples; the Laguna de Bay samples are different with respect to MgO, Zr and Fe_2O_3. Note that there is a large variation in Sr concentrations; the highest SiO_2 samples have relatively high concentrations of Sr (> 200 ppm)

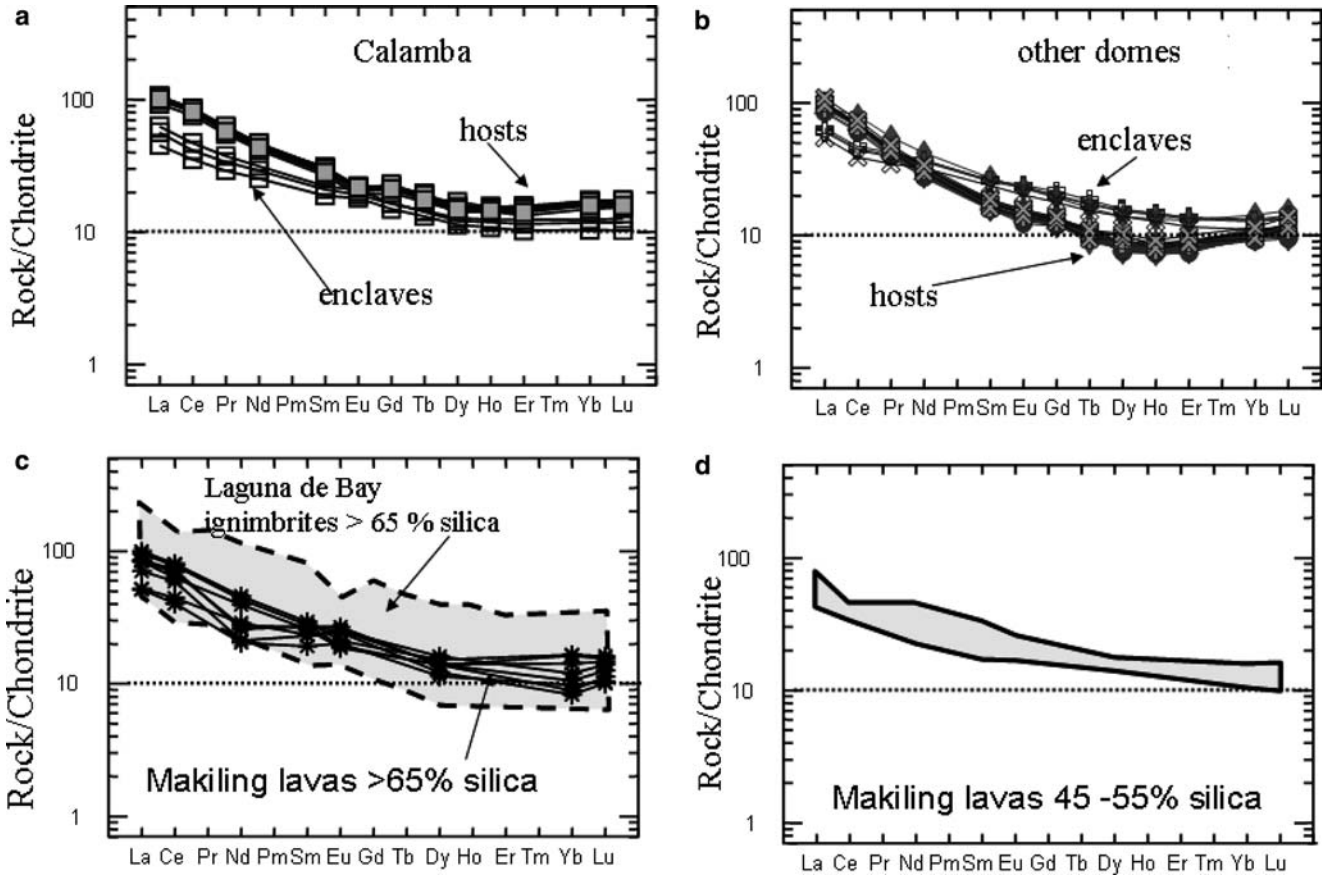

Fig. 6 Chondrite-normalized (Sun and McDonough 1989) REE diagram showing **a** variation in the Calamba Dome, **b** variation in all other domes, **c** variation in the Makiling lavas (data points) and Laguna de Bay ignimbrites with greater than 65 wt% SiO_2 (outlined in a *dashed line*), **d** variation of Makiling lavas with 45–55 wt% SiO_2 (outlined in a *solid line*). Note the similarity in the silicic lavas and host samples for the dome, particularly the Calamba Dome and the similarity of mafic samples from Makiling and the mafic enclaves. Although there is some overlap, the Laguna de Bay silicic samples are distinctly higher in all REEs

Unocal data and unpublished analyses done at the MSU (available as an electronic supplement). Chemical analyses of the Laguna de Bay ignimbrites are from unpublished analyses done at the MSU (available as an electronic supplement). Chemical variations within the mafic enclaves and silicic host of the domes overlap with the chemical variations within the Makiling lavas. This is best displayed in Figs. 4 and 5, which show alkalis, MgO, Fe_2O_3, Zr and Sr variations with SiO_2. The composition of the mafic enclaves and host compositions of the domes are very similar to the compositions of the Makiling lavas. However, the compositions of pumice fragments from Laguna de Bay ignimbrites are different from the domes. This is best documented in Figs. 5 and 6, which show distinct differences in MgO, Fe_2O_3, Zr, Sr and the rare earth elements (REEs) in the domes and ignimbrites. Also, the domes and Makiling lavas contain similar trends, except for the much larger variation in Sr in the intermediate compositions in the Makiling lavas (Fig. 5c). The most striking aspect of the Sr variation is the high concentrations for relatively high SiO_2 values (>200 ppm). The high Sr concentrations and lack of any Eu anomaly precludes any significant plagioclase fractionation.

The REE distribution of the host lavas from the domes is similar except for the Calamba Dome (Fig. 6a). All are characterized by a well-developed concave upward trend in the middle REEs (Fig. 6a, b), a middle rare earth depletion pattern. This pattern is subdued in the Calamba Dome. High silica lavas from Makiling contain a few samples that have a slight concave upward pattern (Fig. 6c), but most do not. Most of the Laguna de Bay silicic samples contain distinctly higher concentrations of REEs (Fig. 6c). The mafic enclaves from the domes are similar to the mafic portions of the Makiling lavas (Fig. 6d).

Spider diagrams normalized to primitive mantle (Sun and McDonough 1989) show that all silicic samples are depleted in Nb and Ti, the characteristic subduction signature (Fig. 7). The domes and Makiling silicic lava samples have very similar patterns (Fig. 7a–c), whereas the silicic Laguna de Bay ignimbrites have distinctly higher values of all elements on these diagrams. The enclaves from the domes are similar to the more mafic Makiling lavas (Fig. 7d).

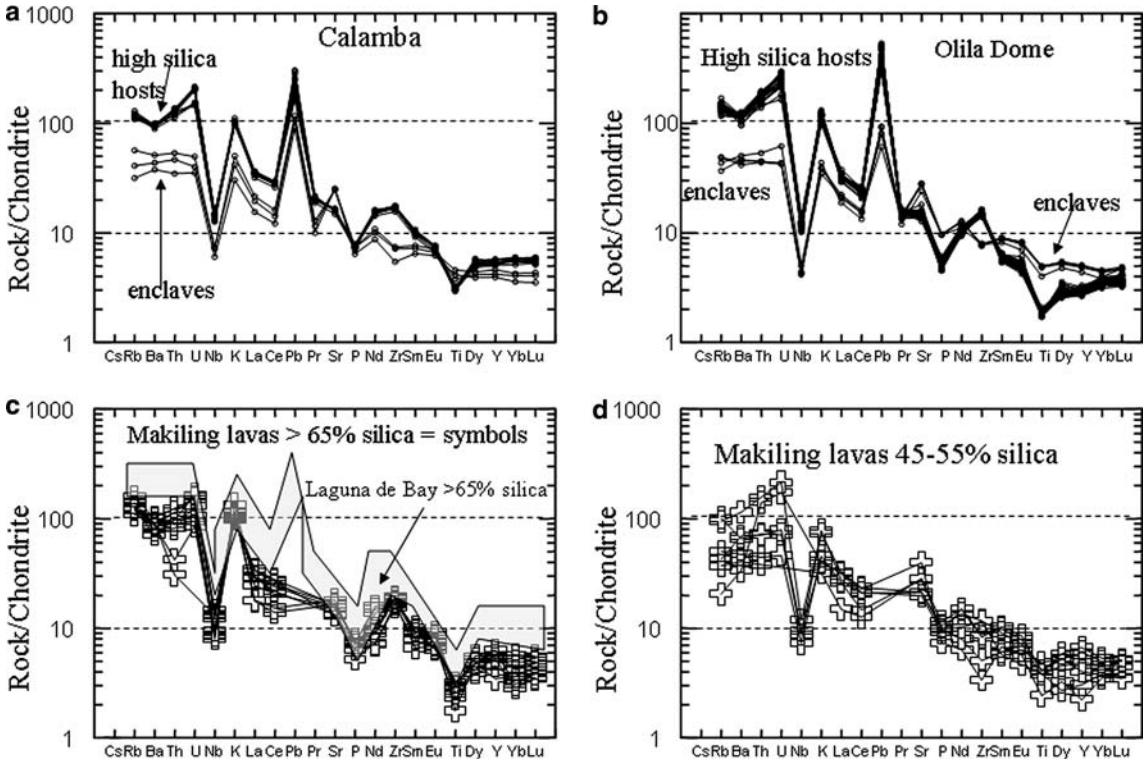

Fig. 7 Primitive mantle-normalized (Sun and McDonough 1989) REE diagrams showing **a** Calamba Dome; **b** all other domes; **c** silicic (>65 wt% silica) for Makiling lavas (data points) and Laguna de Bay ignimbrites (*shaded area*) and **d** Makiling lavas with 45–55 wt% silica

Age constraints

$^{40}Ar/^{39}Ar$ ages were determined for five domes: Mt. Bijang, Calamba, Tanauan Hill, Olila and Mt. Bulalo (Table 5). All are plateau ages. Two samples had four replicates each and yielded internally reproducible results. The Bulalo Dome has an eruptive age of 15 ± 7 ka and the Olila Dome has an eruptive age of 11 ± 8 ka. These domes are adjacent to one another (Fig. 3) and are considered identical in age. For Tanauan Hill and Mt. Bijang, only one $^{40}Ar/^{39}Ar$ age spectrum from hornblende was determined, and we are less confident that the ages truly represent the eruption age. The apparent eruption age for Tanauan Hill is 43 ± 17 ka and Mt. Bijang is 66 ± 14 ka. The eruption age defined by plagioclase for the Calamba Dome is difficult to determine because the age spectrum contains two plateaus. The first plateau is consistent with an 80 ka age, whereas the second plateau is consistent with a 250 ka age. Either could represent the eruption age of the unit, but the plateaus could also result from excess argon (the 250 ka plateau) or argon gain (the 80 ka plateau).

All the domes are relatively young, with the possible exception of Calamba. Both Bulalo and Olila Domes are between 22 and 3 ka with good age constraints. These ages are consistent with the well-preserved morphology of the domes, their glassy matrix texture and the lack of any overlying units. The ages of other domes are not as well constrained, but they most likely erupted <250 ka based on the available age information and their relatively well-preserved morphology. The age of the Makiling lavas is poorly constrained (J.B. Cruz, unpublished thesis). Dates of 510–180 ka have recently been reported (Sudo et al. 2001). However, unpublished U/Pb SHRIMP analyses of zircons from cores recovered from the Mak-Ban geothermal field southeast of Makiling provide evidence that the entire edifice is significantly younger than 350 ka. Two thick rhyolitic ash flow tuff sequences intersect by drilling at depths of about 1 and 1.5 km yielded U/Pb zircon SHRIMP ages of 350 and 500 ka, respectively (J. Lowenstern, personal communication). These units are not exposed at the surface. However, their major element chemistry is similar but more evolved than surface dacite lavas and domes. Considering their stratigraphic position and thickness (locally >200 m), these silicic ash flows probably represent caldera-related deposits that predate the Makiling episode of volcanism (Dimabuyu et al. 2004).

The Laguna de Bay ignimbrites have reported radiocarbon ages from 27 to 50 ka (Catane and Arpa 1998; Arpa et al. 1999a; Catane et al. 2004). However, the upper limit of these ages is poorly constrained due to the limits of radiocarbon dating.

Oxygen isotope data

Data were collected from magnetite and hornblende grains from Calamba, Bijang and Bulalo Domes in order to determine the whole rock $\delta^{18}O$ values for each dome

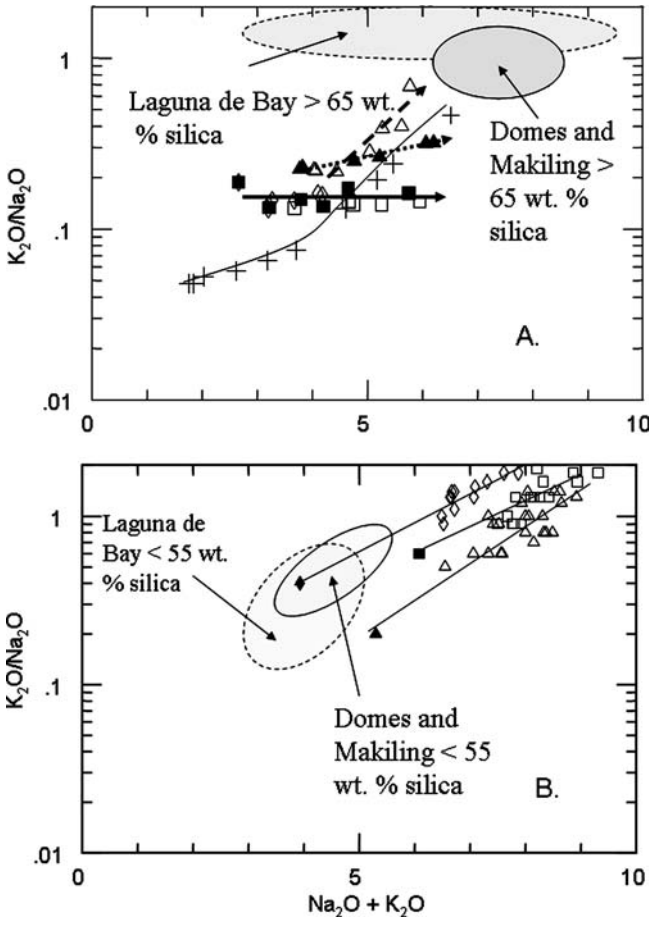

Fig. 8 **a** K_2O/Na_2O versus $K_2O + Na_2O$ plots showing the composition of the silicic samples from the domes, Makiling lavas and Laguna de Bay ignimbrites compared to experimental melt compositions from melting of primitive basalts and andesites. *Open triangle with dashed line* is a starting composition of an Mg-rich andesite at 0.1 MPa; *closed triangle with dotted line* is a starting composition of an Mg-rich andesite at 200 MPa; *open squares* are starting compositions of Medicine Lake basalts at 200 MPa (Grove et al. 2003). *Closed squares* and *closed diamonds* are starting compositions of primitive basalts from Mt. Shasta with 3.8 and 5.0 wt% H_2O, respectively (Müntener et al. 2001). The *pluses with a line drawn through them* is a starting composition of a tholeiitic basalt with extreme fractional crystallization/partial melting with about 3.5% liquid remaining at the highest K_2O/Na_2O values (Villiger et al. 2004). Note that high K_2O/Na_2O samples are not produced by fractional crystallization or partial melting of primitive basalt or Mg-rich andesites. **b** K_2O/Na_2O versus $K_2O + Na_2O$ plots showing the composition of the samples from the domes, Makiling lavas and Laguna de Bay ignimbrites (*shaded areas*) with less than 55 wt% SiO_2 compared to experimental data from Sisson et al. (2005) for melting high-K basalts. *Solid symbols* are the high-K basaltic starting materials; *open symbols* are partial melts produced under various conditions and melt fractions (12–34%). *Lines* connect the same starting compositions with different experimental conditions. Percent liquid in the experiments varied from 34 to 12%. Refer **a** for the compositions of the silicic samples

(Table 4). Minerals were used rather than whole rock because of the secondary hydration of the glass. The $\delta^{18}O$ values collected from each mineral type were similar among the three domes. The magnetite $\delta^{18}O$ values varied by less than 0.12‰ between Bulalo and Bijang and less than 0.5‰ for Calamba. The hornblende $\delta^{18}O$ values were also very similar, with a difference of less than 0.25‰ among all three domes. Whole rock $\delta^{18}O$ values for the domes were calculated assuming equilibrium with the phenocrysts using an assumed temperature of 950°C (Clayton et al. 1989). The calculated whole rock $\delta^{18}O$ values for the three domes were: Bulalo 5.9‰, Calamba 6.29‰ and Bijang 6.06‰. These values are slightly higher than the range of oceanic arcs (4.9–5.8‰) (Eiler et al. 2000). The similarities of the $\delta^{18}O$ values of the mineral phases and the whole rock indicate that the minerals used in the calculations were in equilibrium with each other. As a check on these calculations we calculated the temperature based on amphibole–magnetite equilibrium using the experiments from Chiba et al. (1989) (Table 4). The fractionation factors for amphibole can be assumed to be similar to clinopyroxene (Hoefs 2004). Using the *A* factor from Chiba et al. (1989) the $\delta^{18}O$ of the melt can be calculated from

$$\delta^{18}O\,\text{melt} = \delta^{18}O\,\text{cpx} + (0.061 \times SiO_2\,\text{wt\% minus; } 2.72)$$

(Bindeman et al. 2004). The range from 6.10 to 6.36‰ is similar to the calculations assuming a 950°C temperature (Table 3). This is important because it indicates that the $\delta^{18}O$ oxygen values from the minerals have not been reset and therefore reflect the values of the source rock (Bindeman and Valley 2003). These values preclude a derivation from melting a hydrothermally altered crust and are consistent with a derivation from a mantle-equilibrated source rock either by partial melting or fractional crystallization.

Discussion

The occurrence of abundant silicic rocks in intra-oceanic arc settings has only recently been appreciated (Fiske et al. 2001; Tamura and Tatsumi 2002; Leat et al. 2003; Smith et al. 2003; Tamura et al. 2003; Vogel et al. 2004, 2006). Previously, it was believed that the low abundance of silicic rocks in these settings was due to the absence of continental crust. All the above investigators have attributed the origin of these silicic magmas to the partial melting of crustal rocks with compositions ranging from andesite to amphibolite.

Various workers (Beard and Lofgren 1991; Müntener et al. 2001; Grove et al. 2003; Villiger et al. 2004) have shown that low-K basaltic or low-K andesitic material cannot be a source for these high K_2O/Na_2O calc-alkaline magmas (Fig. 8a). Others have hypothesized that the existence of an evolved crustal component is needed to explain the petrogenesis of these high K_2O/Na_2O calc-alkaline magmas (Patiño Douce and McCarthy 1998; Patiño Douce 1999). However, Sisson et al. (2005), using more evolved basaltic starting compositions, have recently demonstrated that partial melting or advanced fractional crystallization of medium- to high-K basaltic rocks can produce liquids with high K_2O/Na_2O ratios (Fig. 8b).

All the calc-alkaline silicic rocks in the Macolod Corridor contain high alkalis and high K_2O/Na_2O ratios (Fig. 8a). In Fig. 8a, the silicic samples (> 65 wt% SiO_2) from the domes, Makiling lavas and Laguna de Bay ignimbrites are compared to experimental data for crystal fractionation for primitive basalts and primitive andesites (Müntener et al. 2001; Gaetani et al. 2003; Grove et al. 2003; Villiger et al. 2004). The plus symbols in Fig. 8a represent experimental data from nearly perfect fractionation of tholeiitic basalt (the last liquid is less than 3.5% of the original material) with liquids approaching dacite in composition (Villiger et al. 2004). A conclusion from these experiments is that without an evolved source, it is difficult to produce liquids with high alkalis and high K_2O/Na_2O ratios by the partial melting of Mg-rich andesites or primitive basalts.

Recently, Sisson et al. (2005), using evolved basalts in melting experiments, produced melts that have very similar alkalis and K_2O/Na_2O values observed for the silicic rocks in Macolod Corridor (Fig. 8b). One of their starting compositions (Yos-55a) is a gabbro that has alkali concentrations similar to some of the mafic samples in the Laguna de Bay ignimbrite and Makiling basaltic lavas (Fig. 8b). Their experiments demonstrate that the evolved liquids produced by partial melting of medium to high-K basaltic magma or extreme crystal fractionation of moderate to high-K basalt could produce the high K_2O/Na_2O silicic magmas present in the Macolod Corridor. More experiments on high-K andesites are needed.

Our preferred model for the generation of these high-silica magmas is by partial melting of calc-alkaline, mantle-derived, moderate to K-rich crystallized evolved magmas that have ponded and crystallized in the low- to mid-crust. However, partial melting of the lower crustal mid- to high-K mafic rocks could produce these silicic magmas. Tamura and co-workers have discussed in detail the reasons they prefer remelting of crystallized evolved magmas rather than melting of the lower mafic crust for the origin of the rhyolites from the Izu-Bonin Arc and Daisen Volcano, Japan (Tamura and Tatsumi 2002; Tamura et al. 2003). Most of their arguments could be applied to our present study—the inferred large amounts of andesitic plutons in the underlying Luzon crust, energetic considerations of partial melting of hot plutons, the extreme amount of fractional crystallization needed to produce the high K_2O/Na_2O silicic magmas.

It is clear that the Laguna de Bay silicic magmas are chemically distinct from the domes and Makiling lavas, which are nearly identical to each other (Figs. 4, 5, 6, 7). The silicic magmas from Laguna de Bay ignimbrites and the domes have a source distinct from the source of the Makiling lavas. Adjacent to the Macolod Corridor is a sequence of Paleocene–Oligocene San Juan metavolcanics and early to mid-Miocene San Juan quartz diorite (Oles 1991; Sudo et al. 2001), which could potentially be a source for the silicic magmas.

Tamura et al. (2003) have discussed the energy problems of silicic melts production by melting of the cold crust. Remelting of hot, stalled mostly crystalline magmas is an energy efficient process to produce magma (Tamura et al. 2003). Heat for melting is transferred from the emplacement of other mantle-derived magmas to hot plutons. An alternative process is by the extraction of residual melt from stalled, partially crystallized magma (Bachmann and Bergantz 2003, 2004). Each process would produce new magmas of similar compositions.

Few Nd and Sr isotopic studies have been published for igneous rocks in the Macolod Corridor; however, there are some relevant unpublished data. Isotopic studies on Taal lavas and Laguna de Bay pyroclastic deposits showed relatively depleted ratios for both volcanic systems (Mukasa et al. 1994a). For Taal samples, Sr isotopic values range from 0.70443 to 0.70472 and the Nd isotopic values range from 0.51279 to 051285, whereas these ratios in Laguna de Bay samples range from 0.70409 to 70426 and 0.51276 to 0.51285, respectively (Mukasa et al. 1994b). The $^{143}Nd/^{144}Nd$ versus $^{87}Sr/^{86}Sr$ diagram shown in Mukasa et al.'s (1994b) study demonstrates a close cluster of data points similar to the Izu-Honshu Arc of Japan falling well above the bulk earth values. No evidence of evolved continental crust can be observed in these data. Mukasa provided one analysis of a silicic sample from Makiling with an Sr ratio of 0.70417 and Nd ratio of 0.51286 (S.B. Mukasa, personal communication). Seven unpublished Sr isotope analyses of Cristo-Banahaw and five from the Makiling area, including Olila, Bijang and Mabilog Domes (unpublished data, Unocal Philippines, Inc.; analyses done at the UC Santa Barbara by J. Mattinson) were made available. The Cristo-Banahaw data range from 0.70409 to 0.70449, whereas the Makiling data range from 0.70430 to 0.70443. Olila is 0.70430 and Bijang is 0.70420. All these data support the conclusion that the silicic magmas from Makiling had no involvement with the old evolved continental crust—it can be used to support the involvement of young, mantle-derived magmas that intruded in the lower crust. The oxygen isotope compositions show no evidence for hydrothermal alteration, which would support the conclusion that shallowly intruded rocks can be ruled out (these shallowly intruded rocks would be subjected more to hydrothermal alteration and the $\delta^{18}O$ would be shifted to higher values).

Conclusions

The purpose of this study is to document the relative abundance of silicic volcanic rocks (> 65 wt % SiO_2) in the Macolod Corridor of Luzon, Philippines, and to determine their origin. Geochemical data from the silicic domes associated with Mt. Makiling and the ash flow tuffs from Laguna de Bay Caldera reveal compositional differences, demonstrating that these units cannot be genetically related. However, the silicic domes and lavas

from Makiling Volcano have nearly identical trace element and major element trends and are considered part of the same magmatic system. Older rhyolitic rocks represented by core samples from 1 and 1.5 km depth beneath Makiling Volcano are also chemically similar. Alteration of these rocks precludes a detailed interpretation of their chemical affinities; nevertheless, the thickness of these rocks demonstrates a significant abundance of silicic rocks in the area. Recent experimental results (Sisson et al. 2005) have shown that the partial melting of moderate to K-rich basaltic rocks can produce high K_2O/Na_2O silicic magmas. Our conclusion is that the silicic magmas were produced by partial melting of mantle-derived, evolved and crystallized ponded calc-alkaline magmas. Alternatively, the silicic magmas could be produced by melt extraction from these partially crystallized magmas. The generation of silicic magmas in island arcs in the absence of evolved continental crust represents the formation of continental crust.

Acknowledgements We gratefully acknowledge the Philippine Institute of Volcanology and Seismology (PHIVOLCS) and the National Institute of Geological Sciences (NIGS), University of the Philippines—Diliman, Philippines, for continued support of this project. Part of this research was done while one of us (TAV) was a visiting professor at NIGS. Both PHIVOLCS and NIGS provided transportation and other logistical support for the fieldwork. Jake Lowenstern provided SHRIMP Pb/U zircon analyses and interpretation. Sam Mukasa made available unpublished Sr isotopic data. Unocal Philippines, Inc., provided support for the Ar/Ar and Pb/U zircon analyses and also made available drill core samples and unpublished chemical analyses. Oxygen isotopes were measured in John Valley's laboratory by Jonathan Eaton. Ilya Bindeman provided insight into interpreting the oxygen isotopic data. The paper was considerably improved by thoughtful reviews by Kent Ratajeski and Ilya Bindeman.

References

Aquino DJP (2004) Surface structure analysis for the Bulalo geothermal field: possible implications to local and regional tectonics. MS, University of the Philippines, National Institute of Geological Sciences, Diliman, p 116

Arpa MCB, Catane SG, Mirabueno MHH (1999a) Identification of large-scale eruptions of Laguna caldera from Geologic mapping of volcanic deposits found in Rizal province, Metro Manila, and adjacent areas. Philippine Institute of Volcanology and Seismology, Diliman

Arpa MCB, Catane SG, Mirabueno MHH, Bornas MAV (1999b) Identification of large-scale eruptions of Laguna caldera from geologic mapping of volcanic deposits found in Rizal province, Metro Manila and adjacent areas. Philippine Institute of Volcanology and Seismology, Diliman

Bachmann O, Bergantz GW (2003) Rejuvenation of the Fish Canyon magma body: a window into the evolution of large-volume silicic magma systems. Geology 31:789–792

Bachmann O, Bergantz GW (2004) On the origin of crystal-poor rhyolites: extracted from batholithic crystal mushes. J Petrol 45(8):1565–1582

Bacolcol T (2003) Etude géodésique de la faille Philippine dans les Visayas. These de Doctorat, Institut de Physique du Globe de Paris, Paris, p 208

Beard JS, Lofgren GE (1991) Dehydration melting and water-saturated melting of basaltic and andesitic greenstones and amphibolites at 1, 3, and 6.9 kb. J Petrol 32:365–401

Besana GM et al (1995) The shear wave velocity structure of the crust and uppermost mantle beneath Tagaytay, Philippines inferred from receiver function analysis. Geophys Res Lett 22:3143–3146

Bindeman IN, Valley JW (2003) Rapid generation of both high- and low- $\delta^{18}O$, large-volume silicic magmas at the Timber Mountain/Oasis Valley caldera complex, Nevada. Geol Soc Am Bull 115:581–595

Bindeman IN, Ponomareva VV, Bailey JC, Valley JW (2004) Volcanic arc of Kamchatka: a province with high- $\delta^{18}O$ magma sources and large-scale $^{18}O/^{16}O$ depletion of the upper crust. Geochem Cosmochim Acta 68:841–865

Cardwell RK, Isacks BL, Karig DE (1980) The spatial distribution of earthquakes, focal mechanism solutions, and subducted lithosphere in the Philippine and Northeastern Indonesian Islands. In: Hayes DE (ed) The tectonic and geologic evolution of Southeast Asian seas and islands. American Geophysical Union, Washington, pp 1–35

Catane SG, Arpa MCB (1998) Large-scale eruptions of Laguna caldera: contributions to the accretion and other geomorphic developments of Metro Manila and adjacent provinces. Philippine Institute of Volcanology and Seismology, Diliman

Catane SG, Ui T, Arpa MCB, Cabria HB, Taniguchi H (2004) Potential hazards from the youngest explosive eruptions of Laguna Caldera to metropolitan Manila, Philippines. Western Pacific Geophysics Supplement 85:V33A-89

Chiba H, Chacko T, Clayton RN, Goldsmith JR (1989) Oxygen isotope fractionations involving diopside, forsterite, magnetite and calcite. Geochim Cosmochim Acta 53:2985–2995

Clayton RN, Goldsmith JR, Mayeda TK (1989) Oxygen isotope fractionation in quartz, albite, anorthite, and calcite. Geochim Acta Cosmochim 53:725–733

Cobbing EJ, Pitcher WS (1983) Andean plutonism in Peru and its relationship to volcanism and metallogenesis at a segmented plate edge. Mem Geol Soc Am 159:277–291

Defant MJ, Deboer J, Oles D (1988) The Western Central Luzon Volcanic Arc, the Philippines: two arcs divide by rifting? Tectonophysics 45:305–317

Defant M, Jacques D, Maury RC, Boer JD, Joron JL (1989) Geochemistry and tectonic setting of the Luzon Arc, Philippines. Geol Soc Am Bull 101:663–672

DePaolo DJ (1981) Trace element and isotopic effects of combined wallrock assimilation and fractional crystallization. Earth Planet Sci Lett 53:189–202

Dimabuyu AJ, Stimac JA, Sugiaman F (2004) Detailed stratigraphy of the Bulalo Geothermal Field. A tribute to Dr. Roger Datuin, Association of Filipinos for the Advancement of Geoscience, p 68

Eiler JM, Crawford A, Elliott T, Farley KA, Valley JW, Stolper EM (2000) Oxygen isotope geochemistry of oceanic arc lavas. J Petrol 41:229–256

Fiske RS, Naka J, Iizasa K, Yuasa M, Klaus A (2001) Submarine silicic caldera at the front of the Izu-Bonin Arc, Japan; voluminous seafloor eruptions of rhyolite pumice. Geol Soc Am Bull 113:813–824

Förster H, Oles D, Knittel U, Defant MJ, Torres RC (1990) The Macolod Corridor—a rift crossing the Philippine Island-Arc. Tectonophysics 183:265–271

Gaetani GA, Kent AJR, Grove TL, Hutcheon ID, Stolper EM (2003) Mineral/melt partitioning of trace elements during hydrous peridotite partial melting. Contrib Mineral Petrol 145:391–405

Grove TL, Elkins-Tanton LT, Parman SW, Chatterjee N, Muntener O, Gaetani GA (2003) Fractional crystallization and mantle-melting controls on calc-alkaline differentiation trends. Contrib Mineral Petrol 145:515–533

Hildreth W, Moorbath S (1988) Crustal contributions to arc magmatism in the Andes of central Chile. Contrib Mineral Petrol 98:455–489

Hoefs J (2004) Stable isotope geochemistry. Springer, Berlin Heidelberg New York

Knittel U, Defant MJ, Raczek I (1988) Recent enrichment in the source region of arc magmas from Luzon island Philippines: Sr and Nd isotopic evidence. Geology 16:73–76

Leat PT, Smellie JL, Millar IL, Larter RD (2003) Magmatism in the South Sandwich Arc. In: Leat PT (ed) Intra-oceanic subduction systems: tectonic and magmatic processes. The Geologic Society, London, pp 285–313

LeBas MJ, LeMaitre RW, Streckeisen A, Zanettin B (1986) A chemical classification of volcanic rocks based on the total alkali silica diagram. J Petrol 27:745–750

Le Rouzic S (1999) Seismotectonique des structures actives dans la zone de relais, Philippines. PhD, Institut de Physique du Globe de Paris, Paris, p 341

Listanco EL (1994) Space-time patterns in the geologic and magmatic evolution of calderas: A case study at Taal Volcano, Philippines. PhD Thesis, University of Tokyo, Earthquake Research Institute, Tokyo, p 184

Martinez MML, Williams SN (1999) Basaltic andesite to andesite scoria pyroclastic flow deposits from Taal caldera, Philippines. J Geol Soc Philipp 54:1–18

Miklius A, Flower MFJ, Huijsmans JPP, Mukasa SB, Casitillo PR (1991) Geochemistry of lavas from Taal volcano, southwestern Luzon, Philippines; evidence for multiple magma supply systems and mantle source heterogeneity. J Petrol 32:593–627

Mukasa SB, Flower MFJ, Miklius A (1994a) The Nd-, Sr- and Pb-isotopic character of lavas from Taal, Laguna de Bay and Arayat volcanoes, southwestern Luzon, Philippines: Implications for arc magma petrogenesis. Tectonophysics 235:205–221

Mukasa SB, Flower MFJ, Miklius A (1994b) The Nd-, Sr- and Pb-isotopic character of lavas from Taal, Laguna de Bay and Arayat volcanoes, southwestern Luzon, Philippines; implications for arc magma petrogenesis; geology and geophysics of the South China Sea and environs. Tectonophysics 235:205–221

Müntener O, Kelemen PB, Grove TL (2001) The role of H_2O during crystallization of primitive arc magmas under uppermost mantle conditions and genesis of igneous pyroxenites: An experimental study. Contrib Mineral Petrol 141:643–658

Oles D (1991) Geology of the Macolod Corridor intersecting the Bataan–Indoro island arc, The Philippines, Manila, Final report for German Research Society Project No. Fo53/16-1 to 2 and German Agency for Technical Cooperation Project No. 85.2522.2-06.100

Patiño Douce AE (1999) What do experiments tell us about the relative contributions of crust and mantle to the origin of granitic magmas? In: Vigneresse JL (ed) Understanding granites: integrating new and classical techniques. Geological Society, London, pp 55–75

Patiño Douce AE, McCarthy TC (1998) Melting of crustal rocks during continental collision and subduction. In: Hacker BR, Liou JG (eds) When continents collide: geodynamics and geochemistry of ultrahigh-pressure rocks. Kluwer, Dordrecht, pp 27–55

Pubellier M, Garcia F, Loevenbruck A, Chorowicz J (2000) Recent deformation at the junction between the North Luzon block and the Central Philippines from ERS-1 Images. Island Arc 9:598–610

Sisson TW, Ratajeski K, Hankins WB, Glazner AF (2005) Voluminous granitic magmas from common basaltic sources. Contrib Mineral Petrol 148:635–661

Smith IEM, Stewart RB, Price RC (2003) The petrology of a large intra-oceanic silicic eruption: the Sandy Bay Tephra, Kermadec Arc, Southwest Pacific. J Volcanol Geotherm Res 124:173–194

Sudo M, Listanco EL, Ishikawa N, Kamata H, Tatsumi Y (2001) K–Ar dating of the volcanic rocks from the Macolod Corridor in Southwestern Luzon, Philippines: toward an understanding of the Quaternary volcanism and tectonics. J Geol Soc Philipp 55:89–104

Sun S, McDonough WF (1989) Chemical and isotopic systematics of oceanic basalts: implications for mantle compositions and processes. In: Norry MJ (ed) Magmatism in the Ocean Basins. Geological Society Special Publications, pp 313–345

Tamura Y, Tatsumi Y (2002) Remelting of an andesitic crust as a possible origin for rhyolitic magma in oceanic arcs: an example from the Izu-Bonin arc. J Petrol 43:1029–1047

Tamura Y, Yuhara M, Ishii T, Irino N, Shukuno H (2003) Andesites and dacites from Daisen volcano, Japan: partial-to-total remelting of an andesite magma body. J Petrol 44:2243–2260

Valley JW, Kitchen N, Kohn MJ, Niendorf CR, Spicuzza MJ (1995) UWG-2, a garnet standard for oxygen isotope ratios: Strategies for high precision and accuracy with laser heating. Geochem Cosmochim Acta 67:3257–3266

Vielzeuf D, Holloway JR (1988) Experimental determination of the fluid-absent melting reactions in the pelitic system. Contrib Mineral Petrol 98:257–276

Villiger S, Ulmer P, Muntener O, Thompson AB (2004) The liquid line of descent of anhydrous, mantle-derived, tholeiitic liquids by fractional and equilibrium crystallization—an experimental study at 1.0 GPa. J Petrol 45:2369–2388

Vogel TA, Patino LC, Alvarado GE, Gans PB (2004) Silicic ignimbrites within the Costa Rican volcanic front: evidence for the formation of continental crust. Earth Planet Sci Lett 226:149–159

Vogel TA et al (2006) Origin of silicic magmas along the Central American volcanic front: Genetic relationship to mafic melts. J Volcanol Geotherm Res (in press)

White AJR, Chappell BW (1983) Granitoid types and their distribution in the Lachlan Fold Belt, southeastern Australia. In: Roddick JA (ed) Circum-Pacific plutonic terranes. Geological Society of America, Boulder, pp 21–34